Journal of Ovonic Research Vol. 16, No. 2, March - April 2020, p. 97 - 106

STUDY THE ROLE OF EFFECTIVE PARAMETERS IN ENHANCEMENT OF THE SILICON SOLAR CELL PERFORMANCE USING PC1D SIMULATION

M. S. AHMED, S. M. AHMAD*, M. SUBHYALJADER
Department of physics, Faculty of Science, University of Mosul, 41002 Mosul, Iraq

The increased spread of the solar cell in the market relies on an improvement of the performance of silicon solar cell which is through study the role of effective parameters and focus on it to improve performance. In this study, detailed modelling of the solar cell was carried out so as to identify key parameters impacting efficiency. The impact of various parameters such as base resistivity, emitter doping concentration, front and rear surface recombination, back surface field, minority carrier lifetime, surface reflection and series and shunt resistance were investigated using PC1D software simulation. We are found that the top doping for emitter, bulk and back surface field were between 1×10^{19} cm^{-3} and 1×10^{20} cm^{-3}. Where, the efficiency can be impacted by 2.7 % through emitter concentration variation, 1.5 % through FSRV, 1% through BSRV, and 1 % through bulk resistivity. The largest variation was observed for the minority carrier lifetime; it was observed that low lifetimes (~ 10-20 μs) are sufficient for efficiency of ~ 18 %. As for the surface reflection is concerned each 10 % increase in absolute reflection results in approximately 2 % efficiency reduction. As the largest variation was observed for the series and shunt resistance; it was observed that low series resistance (~ 0.01) and high shunt resistance (~ 100) are sufficient for the efficiency of ~ 19 %. The results from this simulation found that key parameters to improve the solar cell performance lay by optimizing emitter concentration, reduce surface reflection, series resistance low as possible, and shunt resistance high as possible.

(Received October 28, 2019; Accepted March 13, 2020)

Keywords: Solar cell, Emitter, Reflection, Series resistance, Minority carrier lifetime

1. Introduction

The gross power exhaustion of the world in 2018 was more than 22,000 TWh, furthermore, the statistics exhibit that the request for energy is rising by 2% all over the world [1]. With the existing energy generation infrastructure, almost 87 % is generated through fossil fuels, therefore emits CO_2 and other harmful greenhouse gases. Therefore, development of clean, secure, environmentally sustainable, and affordable energy sources must be the sole priority at this time. Renewable energy resources represent the only viable alternatives to fossil fuels [2]. The obvious choice of a renewable energy source is the Solar cell. Computer simulations play an active role in solar cell research and development. Many new concepts are often complex with a large number of processing steps. The modeling of the fabrication processes can reduce cost and expensive instrumentation time. Additionally, the scientific benefits through the simulation provide essential insights into the physics of solar cell performance, allowing users to scout the wide range of design choices. PC1D is a computer software established for IBM-compatible personal computers, that solve the entirely connected non-linear equations for the quasi-one-dimensional transport of electrons and holes in crystalline semiconductor system, with confirm on solar cell devices [3].

The silicon solar cell is trade-off device where a surface passivation can be improved by decrease surface doping concentration but raises contact resistivity. A shallow junction depth enhances short-wavelength collection efficiency but raises the tendency of shunting [4]. Both open-circuit voltage and short-circuit current density are independent of the wafer thickness for

* Corresponding author: samirasia2013@gmail.com

most thicknesses. Only for wafer thickness, less than 200 mm is a statistically important change in the short-circuit current observed, depending on the type of the passivation layer [5]. Therefore, study the key parameters in making high efficiency silicon solar cell are very important. Several researchers have attempted to study the role of affective parameters on the performance of silicon solar cell. For example, Belarbi et al. [6] made several simulations to see the impact of various parameters on the efficiency of solar cells. They find that the more short n-region thickness the more we have of chance that a large number of electrons leave the cell and contribute to the conduction. As well, that the increase n-region and p-region doping beyond a certain value negatively affects the performance of the solar cell. Hashmi et al. [7] used the PC1D software to simulate p-type mono-crystalline silicon solar cell. The simulation as well provides insight into the range and impact of p-type and n-type doping concentration, diffusion length, texturing and anti-reflection coating. They saw that the textured surface decreases reflection and improves the efficiency of the solar cell at least 1–2%. Also, they found that the best value of p-type doping concentration is 1×10^{17} cm^{-3} and n-type doping concentration is 1×10^{18} cm^{-3}. For, diffusion length optimums value was 200.3 μm. The 2.019 refractive index for the anti-reflection layer and 74 nm thickness is considered as optimum.

In this paper, silicon solar cell device have been simulated using real physical device configurations. This study concentrates on optimization of n+pp+ silicon solar cells by using PC1D simulations.

2. Simulation by PC1D

Effective and precise simulating needs all the parameters of the solar cell to be inserted. In PC1D, the simulation program should put up with a set of standardized guidance's which are: Specification of the structure parameters (like device area, surface texture, optical coating) and Specification of the layer parameters (like band gap, and doping concentration) used for simulations which presented in Table 1.

Fig. 1 illustrates typical solar cell modelling configuration used in the PC1D version 5.9 software. Solar cell performance was modelled as a function of stringent procedure parameters including wafer resistivity, emitter doping concentration, minority carrier lifetime, surface recombination velocity, spectral reflection, and parasitic resistances. Figures 2 exhibit light current voltage (LIV) for a 18.7 % efficient solar cell. The cell exhibited an efficiency of 17.1 % with open circuit voltage of 0.630 V, short circuit current of 36.7 mA/cm^2, and fill factor of 81 %.

Table. 1. Process parameter for the Si solar cell model.

Process Parameter	Value and unit
Device area	10 cm^2
Front surface texture depth	3 μm/ 54.74°
Rear surface optically coated	SiN
Series resistance	0.04 Ω
Shunt resistance	0.01 S
Thickness	200 μm
Dielectric constant	11.9
Band gap	1.124 eV
P-type background doping	$1x\ 10^{16}$ cm^{-3}
N-type doping concentration	$5x\ 10^{20}$ cm^{-3}
P^+ concentration	$1x10^{18}$ cm^{-3}
Minority carrier life time	100 μs
Front surface recombination	10000 cm/s
Rear surface recombination	10000 cm/s

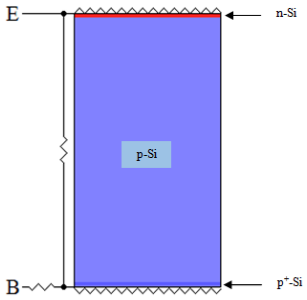

Fig. 1. Solar cell configuration used in PC1D software.

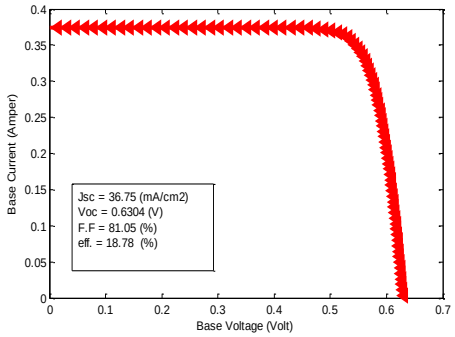

Fig. 2. LIV response of a 18.7 % efficiency solar cell.

3. Simulation results and discussion

3.1. Impact of base resistivity

Base resistivity of the wafer is inherent and depends on the initial doping concentration during the time of its fabrication [8]. It is well known that each cell concept requires a specific base doping concentration to reach its highest efficiency. for instance, several research groups [9–11] have used different quality bulk material manufactured from several methods such as heat exchanger method (HEM), electromagnetic casting (EMC), direct solidification system (DSS) to fabricate high efficiency solar cells. Therefore it is important to examine the effects of bulk resistivity variation on the performance of solar cell. Fig. 3 plots solar cell parameters variation as a function of base resistivity. From the plotted data in Fig. 3a, it can be indicated that the open circuit voltage (V_{oc}) decrease with increase the base resistivity, With almost the same behaviour, the fill factor (FF) changes with the base resistivity (Fig. 3c). While the short circuit current density (J_{sc}) behaves inversely as it increases with increasing resistivity with a slightly increased ratio after 2 Ω.cm as shown in Fig. 3b. The plotted data in figure 3d inferred that the starting wafer base resistivity should be in ~ 0.1-3 Ω.cm range and reveals a sharp maximum at ~ 0.5 Ω.cm. Because of heavily bulk doping (resistivity less than 0.5 Ω.cm), lead to increase carrier recombination that leads to reduced minority carrier lifetime and diffusion length, subsequently reduce the performance of the solar cell. While, lightly doping (resistivity more than 3 Ω.cm) lead to increase series resistance and emitter junction depth. Solar cells with deeper junction will need to longer minority carrier lifetime to obtain better performance. According to our resistivity range, the overall impact on efficiency is limited (~ 1 % absolute reduction in efficiency).

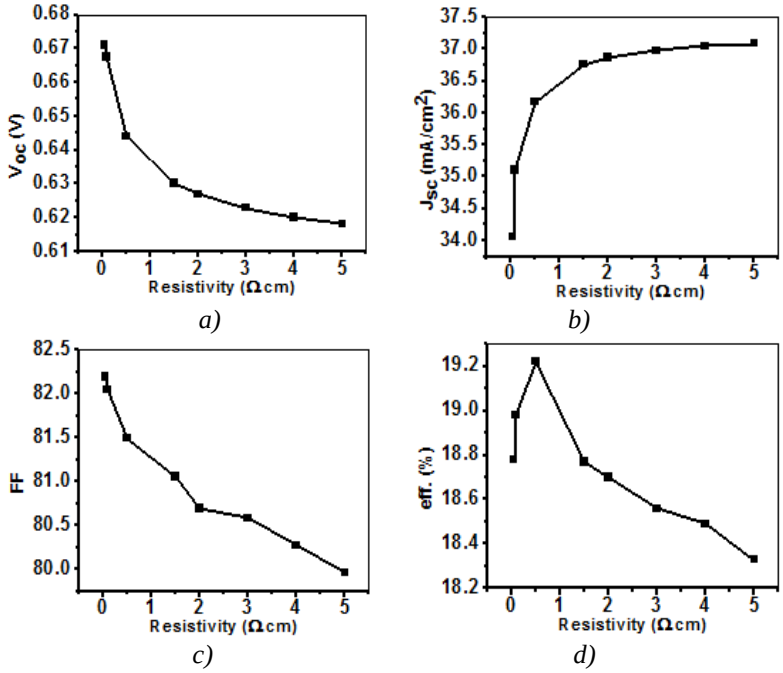

Fig. 3. Show the solar cell parameters variation (V_{oc} (a), J_{sc} (b), FF (c), and efficiency (d) as a function of bulk resistivity.

3.2. Impact of Emitter Doping Concentration

Diffusion to create the emitter (p-n junction) is maybe the most significant stride in solar cell manufacturing [12]. Depend on experimental operation parameters like temperature, time, gas flow rate, structure, emitter doping concentration can be changed over a broad range. Thus, it is essential to appreciate its impact on efficiency. For simulations, the n-layer doping concentration was changed over six orders of magnitude from 5×10^{16} to 1×10^{22} cm^{-3}; these values are fine within empirically obtainable values.

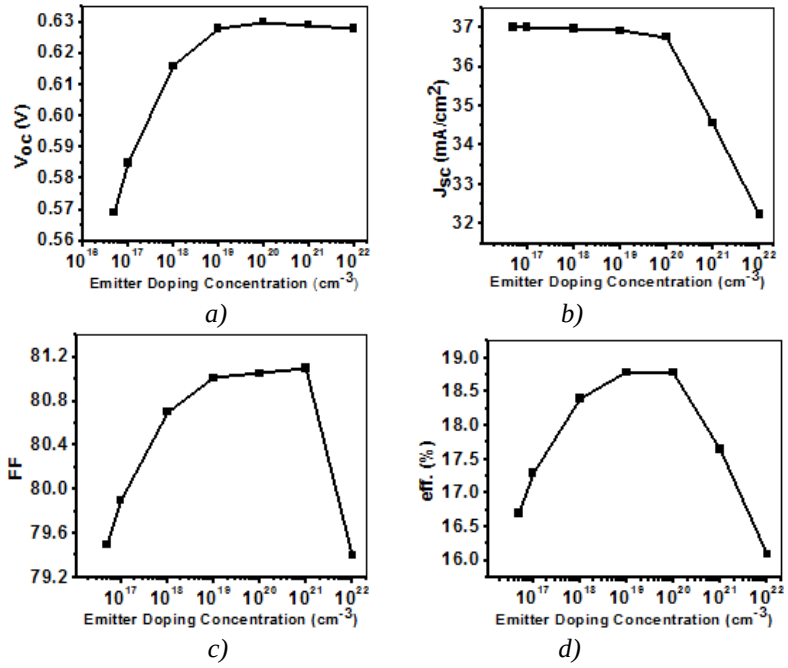

Fig. 4. Show the solar cell parameters variation (V_{oc} (a), J_{sc} (b), FF (c), and efficiency (d) as a function of emitter doping concentration.

Fig. 4 plots solar cell parameters variation as a function of n layer doping concentration. starting, from Fig. 3a it can be shown that the open circuit voltage rapid raising with increase the doping concentration even $1x10^{19}cm^{-3}$ after that slow reduction in the open circuit voltage. While the reduction in the short circuit current density, as shown in figure 3b, is slow to decrease even $1x10^{20}cm^{-3}$ then rapid reduction with an increase in the emitter doping concentration. As for figure 4c and d, it is describes maximum values in fill factor and efficiency for emitter doping varying between $1x10^{19}$ and $1x10^{20}cm^{-3}$. This is attributed to enhanced surface recombination velocity in heavily-doped emitter layers. In accord with emitter doping concentration range, the total impact on efficiency is quite touching (~ 2.7 % absolute reduction in efficiency)

3.3. Impact of Back Surface Field (BSF) Doping Concentration

The solar cell with the back surface field has a better spectral response than that of the solar cell without a back surface field [13]. The BSF amend significantly the summation of carriers with long wavelengths of the solar spectrum by decreasing recombination at the backside of the BSF solar cell [14]. Hence, the short-circuit current density rises. The open-circuit voltage is also improved because short-circuit current density rise and the supplemented potential energy between p and p^+ layers [15]. Figure 5 plots solar cell parameters variation as a function of BSF doping concentration in 10^{16} to 10^{20} cm^{-3} ranges. The simulated data in Fig. 5 for the four parameters reveals a maximum for doping levels in ~ 10^{19}- 10^{20} cm^{-3} range. It is seen that the solar cell parameters raise quickly as the doping concentration is raised to $1.5x10^{19}$ cm^{-3}; at higher doping concentration, the performance starts with stability. It is worth mentioning that in addition to the doping concentration the width of the back surface field region is a vital parameter to reach an optimized pp+ interface with low surface recombination velocity [16]. In accord with BSF doping concentration range, the total impact on efficiency is limited (~ 1 % absolute reduction or elevation of efficiency)

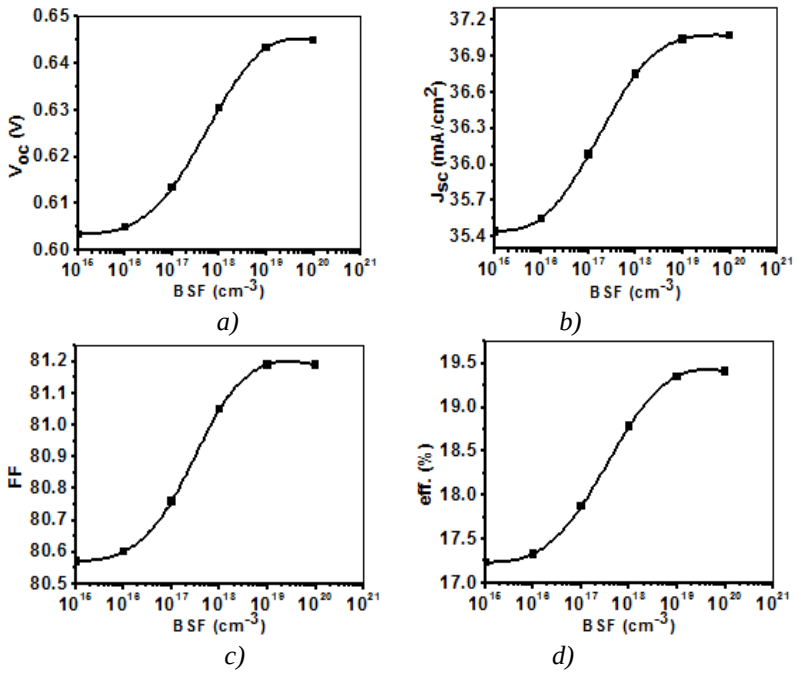

Fig. 5. Show the solar cell parameters variation (V_{oc} (a), J_{sc} (b), FF (c), and efficiency (d) as a function of BSF doping concentration.

3.4. Impact of Front and Back Surface Recombination Velocity

Generally, the recombination carriers depend essentially on the steps of cell material manufacturing like the surfaces and the bulk recombination. Indeed, the solar cell surface is a site of particularly high recombination due to a severe disruption of the crystal lattice. Besides, the

recombination phenomenon has a crucial impact on both open circuit voltage and short circuit current density. Electrons and holes can recombine at the surfaces of a silicon wafer because of unsaturated chemical bonds (dangling bonds). These dangling bonds generate energy levels within the band gap of silicon where charge carriers recombine at a speed referred to as the surface recombination velocity (SRV). In this section, the solar cell performance variation as a function of front surface recombination velocity (FSRV) and back surface recombination velocity (BSRV) has been simulated.

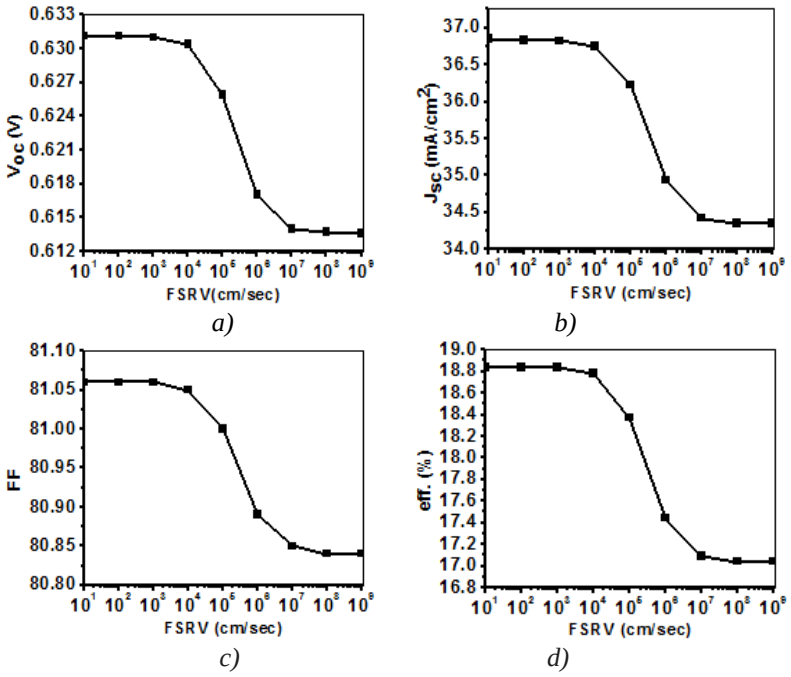

Fig. 6. Show the solar cell parameters variation (V_{oc} (a), J_{sc} (b), FF (c), and efficiency (d) as a function of front surface recombination velocity.

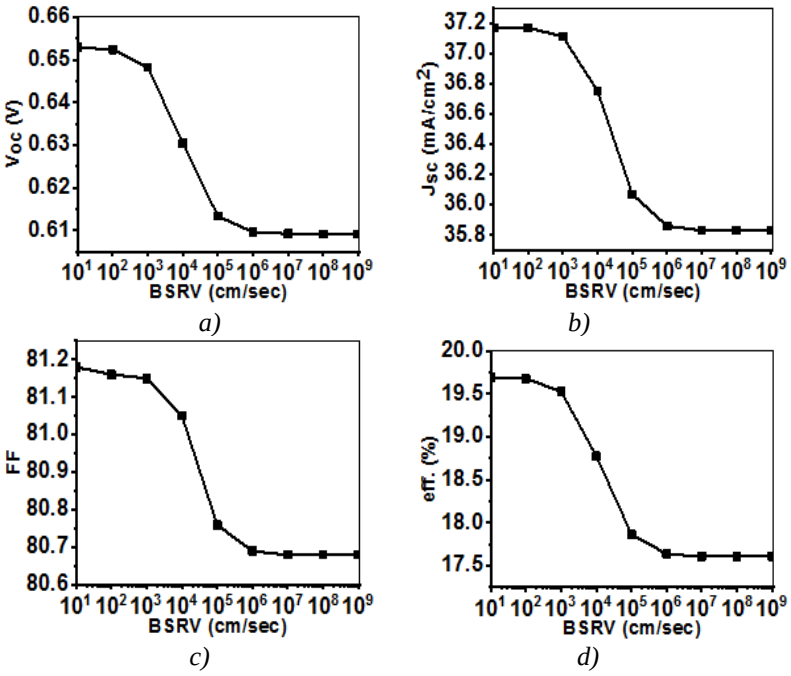

Fig. 7. Show the solar cell parameters variation (V_{oc} (a), J_{sc} (b), FF (c), and efficiency (d) as a function of back surface recombination velocity.

Fig. 6 plots solar cell parameters variation as a function of FSRV in the range of 10^1 to 10^9cm/s. The simulated data in Fig. 6 reveals that as the front surface recombination velocity increases, the value of the four parameters rapidly decreases even FSRV is 10^7 after that less sensitive due to the carrier starts to full recombining at the defect surfaces. In accord with FRRV range, the total impact on efficiency is limited (~ 1.5 % absolute reduction in efficiency). Fig. 7 plots the solar cell performance as a function of BSRV in the range of 10^1 to 10^9cm/s. The simulated data in Fig. 7 reveals that as the back surface recombination velocity increases the value of the four parameters decreases but the difference in magnitude is little bigger in comparison to those that correspond to the front surface recombination velocity. This attributed to that the effect of BSRV in high minority carrier lifetime solar cells is bigger because the generation rate becomes higher at the back surface. While the minority carriers which are generated close to the back surface are not able to reach the junction if the wafer is thick enough[17]. In accord with BRRV range, the total impact on efficiency is limited (~ 1 % absolute reduction in efficiency).

3.5. Impact of Surface Reflection

The silicon surface reflected 30% of the incident light, which could contribute to photo-generated current, is lost by front reflection [18]. Therefore, reduce the current density. Figure 8 plots the solar cell performance as a function of front surface reflection in the range of 0% to 40%. The figure 8a reveals that the contribution for efficiency diminishment comes from the loss in V_{oc}, which decreased by nearly 3 mV for each 10 % increase in absolute reflection. While, the figure 8b reveals that the main contribution for efficiency diminishment comes from the loss in J_{sc}, which decreased by 4 mA/cm^2 for each 10 % increase in absolute reflection. While the figure 8c reveals that the fill factor is not affected by increased reflection and therefore it has a little contribution to efficiency loss. From the figure 8d, surface reflection is concerned each 10 % increase in absolute reflection results in approximately 2 % efficiency reduction.

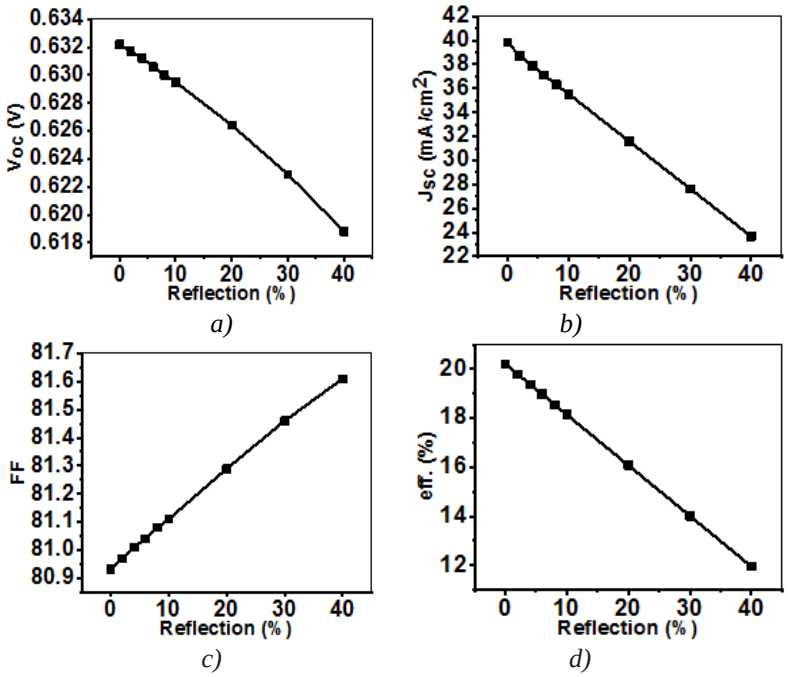

Fig. 8. Show the solar cell parameters variation (V_{oc} (a), J_{sc} (b), FF (c), and efficiency (d) as a function of surface reflection.

3.6. Impact of Minority Carrier Lifetime

The minority carrier lifetime (τ) is critically related to the efficiency of a solar cell. If the lifetime is low, the carriers recombine before collection by the junction, thus, efficiency is

reduced. Fig. 9 plots the parameters of the solar cell as a function of minority carrier lifetime in the range of 0.1 μs to 200 μs. The four parameters increase rapidly as a function of lifetime over a narrow range from ~ 0.1 to 20 μs. At higher lifetimes, the four parameters enhancement is marginal. This is because for 200-μm thick wafer solar cells, all minority carriers can reach front surface junction as long as their lifetime is larger than 10 μs which corresponding 170 μm diffusion length (L_d) ($L_d = \sqrt{D\tau}$, D is diffusion coefficient) which is necessary to ensure a high photo generated current.

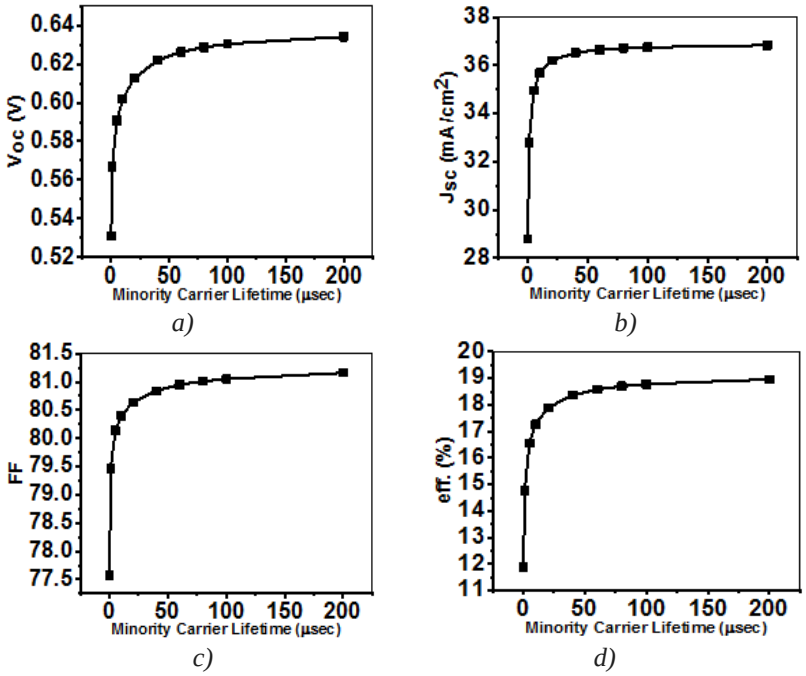

Fig. 9. Show the solar cell parameters variation (V_{oc} (a), J_{sc} (b), FF (c), and efficiency (d) as a function of minority carrier lifetime.

3.7. Impact of Series and hunt Resistance

The series and shunt resistances affect mainly the fill factor and therefore affect the efficiency of the solar cell. The series resistance is the sum of resistance due to all the components (base, emitter, metallic contacts of the front- and a back surface and further circuit resistances from connections and terminals) that come in the path of current. The shunt resistance is essentially bred by leakage currents across the p-n junction because of impurities close to the junction, which produce partial shorting of the junction, especially close to the cell edges. Figs. 10 and 11 plots the solar cell parameters variation as a function of series and shunt resistances. For series resistance, the efficiency decreases slowly as a function of series resistance over a range from ~ 0.001 to 0. 1 Ω. At higher series resistances, the efficiency breakdown is wide as shown in figure 10d. This is because of the drops in FF as shown in figure 10c. While the figure 10a reveals that the open-circuit voltage is not affected by increased series resistance and therefore it doesn't a contribution to efficiency loss. As for figure 10b that reveals that the short-circuit current density has little affected by increases series resistance and therefore it has a very little contribution to efficiency loss. For shunt resistance, the efficiency increases rapidly as a function of shunt resistance over a range from ~ 1 to 100 Ω. At higher shunt resistances, the efficiency enhancement is marginal as shown in figure 11d. This is because of the enhancement in FF and V_{oc} as shown in Fig. 11c and a. While the figure 11b exhibits that the J_{sc} has little affected by increased shunt resistance and therefore it has weak a contribution to efficiency loss. Therefore, this implies that the series resistance should be as low as possible and shunt resistance should be as high as possible.

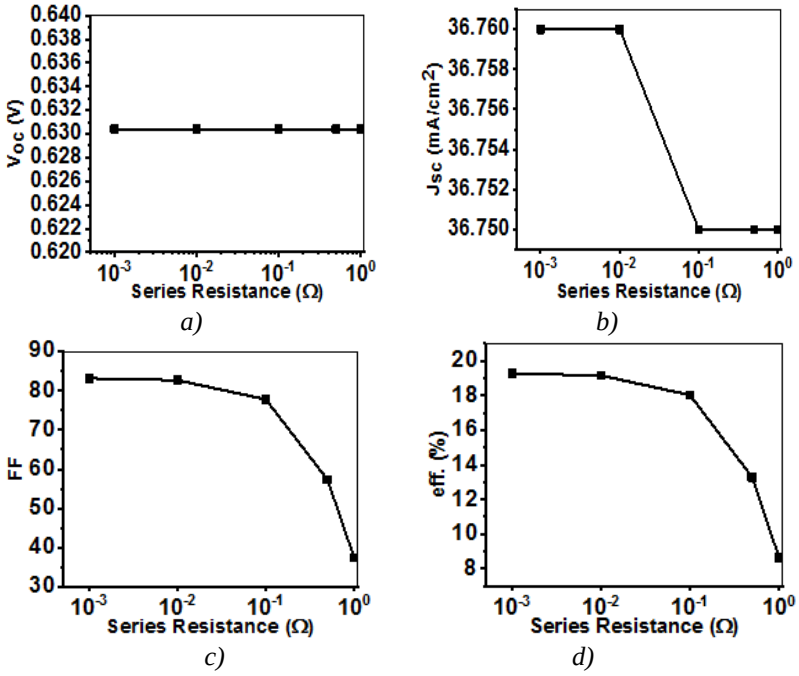

Fig. 10. Show the solar cell parameters variation (V_{oc} (a), J_{sc} (b), FF (c), and efficiency (d) as a function of series resistance.

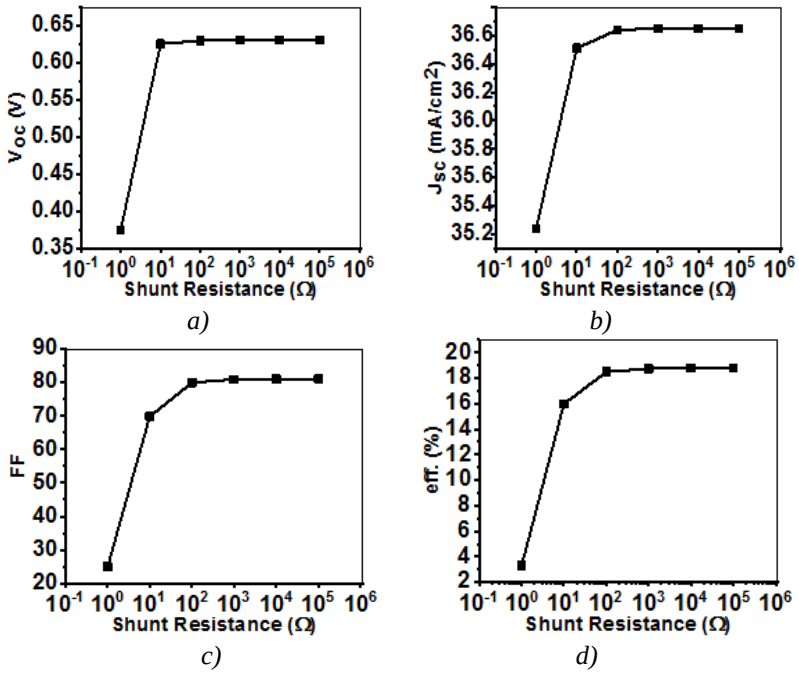

Fig. 11. Show the solar cell parameters variation (V_{oc} (a), J_{sc} (b), FF (c), and efficiency (d) as a function of shunt resistance.

4. Conclusions

Critical process variables influencing silicon solar cell performance have been simulated. The PC1D program was used to simulate for 18.7 % solar cell efficiency; this range was typical of industrially produced solar cells. It was noted that the best doping for n-layer, substrate and BSF were between 1×10^{19} cm^{-3} and 1×10^{20} cm^{-3}. Where, the efficiency can be impacted by 1%, 2.7 %,

1.5 % and 1 % through base resistivity, emitter concentration variation, FSRV, and BSRV respectively. The largest variation was observed for the minority carrier lifetime; it was observed that low lifetimes (~ 10-20 μs) are sufficient for efficiency of ~ 18 %. As for the surface reflection is concerned each 10 % increase in absolute reflection results in approximately 2 % efficiency reduction.

As the largest variation was observed for the series and shunt resistance; it was observed that low series resistance (~ 0.01) and high shunt resistance (~ 100-1000) are sufficient for the efficiency of ~ 19 %. The results of our simulation studies show that it is probably to suggest these design parameters for silicon solar cell manufacturing. Our results also supply critical insight concerning the identify key parameters impacting efficiency.

References

[1] World Power consumption | Electricity consumption | Enerdata: https://yearbook.enerdata.net/electricity/electricity-domestic-consumption-data.html. [Accessed: 22-Aug-2019].

[2] M. Balat, Energy Exploration and Exploitation. **23**(2), 141(2005).

[3] P. A. Basore, D. A. Clugston, Proceeding of the 25th IEEE Photovoltaic Specialists Conference, (1996).

[4] P. Doshi , J. Mejia, K. Tatel, S. Kamra, A. Rohatgi, Proceeding of the 25th IEEE Photovoltaic Specialists Conference, 1996.

[5] A. W. Tool, C. J. J., Burgers, A. R., Manshanden, P., Weeber, Proceeding of the 17th European Photovoltaic Solar Energy Conference, 2001.

[6] M. Belarbi, A. Benyoucef, B. Benyoucef, Advaned Energy: An International Journal (AEIJ) **1**(3), 1 (2014).

[7] G. Hashmi, A. Rafique, A. Mahbubul, H. Habibur, Silicon, 2018.

[8] C. S. Solanki, Solar photovoltaics Fundamentals, Technologies and applications, PHI Learning Privete Limited, Delhi, 2011.

[9] A. Rohatgi, S. Narasimha, S. Kamra, P. Doshi, C. P. Khattak, K. Emery, H. Field, Proceeding of the 25th IEEE Photovoltaic Specialists Conference, 1996.

[10] P. Barton, G. Coletti, T. Veltkamp, and K. Nakagawa, Proceeding of the 25th European Photovoltaic Solar Energy Conference, (2010).

[11] J. Zhao, A. Wang, M. A. Green, F. Ferrazza, Applied Physics Letters. **73**(14), (1998).

[12] S. Sepeai, S. H. Zaidi, M. K. M. Desa, M. Y. Sulaiman, N. A. Ludin, M. A. Ibrahim, K. Sopian, Journal of Energy Technologiesand Policy **3**(5), 1 (2013).

[13] S. H. Lee, D. W. Lee, E. G. Shin, S. H. Lee, Current Photovoltaic Research **4**(1), 12 (2016).

[14] S. H. Ahmad, S. M., Leong, C. S., Winder, R. W., Sopian, K., Zaidi, Journal of Electronic Materials **42**(9), (2019).

[15] S. Tobbeche, M. N. Kateb, Materials Science **21**(4), 491(2015).

[16] J. Szlufcik, S. Sivoththaman, J. F. Nijs, R. P. Mertens, R. Van Overstraeten, Proceedings of the IEEE **85**(5), 711 (1997).

[17] V. Budhraja, N. M. Ravindra, D. Misra, Emerging Materials Research **1**(EMR1), 25 (2011).

[18] R. Sharma, A. Gupta, and A. Virdi, Journal of Nano- and Electronic Physics **9**(2), (2019).